Available online at www.sciencedirect.com
SCIENCE DIRECT
Applied Catalysis B: Environmental 62 (2006) 359–368
APPLIED CATALYSIS B: ENVIRONMENTAL
www.elsevier.com/locate/apcatb

Model bimetallic Pd-Ni automotive exhaust catalysts: Influence of thermal aging and hydrocarbon self-poisoning

A.B. Hungría [a], J.J. Calvino [b], J.A. Anderson [c], A. Martínez-Arias [a,*]

[a] *Instituto de Catálisis y Petroleoquímica, CSIC, C/Marie Curie 2, Campus Cantoblanco, 28049 Madrid, Spain*
[b] *Dpto. de Ciencia de los Materiales e Ingeniería Metalúrgica y Química Inorgánica, Facultad de Ciencias, Universidad de Cádiz, 11510 Puerto Real, Cádiz, Spain*
[c] *Surface Chemistry and Catalysis Group, Department of Chemistry, University of Aberdeen, AB24 3UE Scotland, UK*

Received 1 July 2005; received in revised form 26 August 2005; accepted 2 September 2005
Available online 11 October 2005

Abstract

Bimetallic Pd-Ni catalysts supported on Al_2O_3 and $(Ce,Zr)O_x/Al_2O_3$ were examined with respect to their catalytic performance for the elimination of CO, NO and C_3H_6 under stoichiometric conditions. The effects of a thermal aging treatment at 1273 K, reactant competition in the presence of the hydrocarbon and the influence of the presence of nickel in the catalyst have been analysed by XRD, HREM, catalytic activity measurements and in situ DRIFTS spectroscopy. Self-poisoning effects, induced by the presence of the hydrocarbon in the reactant mixture, were identified as the main factor affecting the light-off activity. While a Ni-induced preferential interaction between Pd and the Ce-Zr mixed oxide component appears, in general terms, to be beneficial for the catalytic performance of the fresh $(Ce,Zr)O_x/Al_2O_3$-supported bimetallic catalyst, it is shown to be detrimental for the aged system as a consequence of a facilitated degradation of the $(Ce,Zr)O_x$ component and encapsulation of the active palladium particles.

Keywords: Pd-Ni bimetallic catalysts; TWC; CeO_2-ZrO_2; Al_2O_3; CO oxidation; NO reduction; Propene oxidation; XRD; In situ DRIFTS; HREM

1. Introduction

Three-way catalysts (TWC) are widely used to diminish pollutant emissions from gasoline engine powered vehicles [1]. Classical components of these systems usually include Rh, Pt and/or Pd as active metals, ceria as promoter and high surface alumina as the support [1,2]. In modern TWC formulations, the traditional promotion by ceria has been extended to other structurally related oxide systems in order to increase or maintain the durability of the TWC while enhancing oxygen storage capacity (OSC) properties of the catalyst [2,3]. In this respect, Ce-Zr mixed oxide systems, and in particular, in alumina supported Ce-Zr mixed oxide configurations, have been considered as optimum metal supports on the basis of their greater oxygen storage capacity after thermal sintering, which could potentially increase the useful lifetime of the catalytic system [3].

The use of Pd as a single active metal component in TWC has received considerable attention on the basis of economical aspects (the high cost and scarcity of Rh), the availability of cleaner fuels and its remarkable activity for oxidation reactions [1,2,4]. Nevertheless, the increasingly stricter limits imposed worldwide for toxic automobile emissions have forced new demands and requirements in three-way catalysts to be considered. Among them, achievement of lower light-off temperature during the cold start phase is of the greatest relevance, considering that the largest portion of the toxic emission is produced during that period [1]. An interesting approach in these respects consists of promoting Pd with lower cost base metals [2]. Promising results in this sense have been obtained by using Mn, Cr or Cu, which have been attributed to the formation of the corresponding alloys (with consequent perturbation of the Pd electronic properties) or, in the case of Mn, to a mixture of effects involving alloy formation and Pd-MnO_x interactions [5–8]. Another metal that may be considered as a potential promoter of Pd activity for these reactions is Ni. Reports by researchers at Nissan-Japan have shown the beneficial effect of establishing interactions between Pd and

* Corresponding author. Tel.: +34 91 5854940; fax: +34 91 5854760.
E-mail address: amartinez@icp.csic.es (A. Martínez-Arias).

0926-3373/$ – see front matter © 2005 Elsevier B.V. All rights reserved.
doi:10.1016/j.apcatb.2005.09.003

Ni, in particular for enhancing NO_x conversion activities under stoichiometric or rich atmospheres [9,10]. However, the promoting effects of nickel in this type of system, as generally postulated in this type of multicomponent catalyst [4], can strongly depend on the particular configuration of catalyst components present in each case. Thus, recent reports on the same Pd-Ni catalysts that are examined in the present contribution (and which differ from the catalysts of Yamamoto et al. which display well formed nickel aluminate crystals [9,10] in the considerably lower nickel loading and the highly dispersed structures of oxidic nickel entities initially present in our catalysts [11,12]) have revealed that nickel induces mainly a promotion of CO oxidation as a consequence of an indirect favouring of the establishment of contacts between palladium and nanostructured configurations of the Ce-Zr mixed oxide component [11,12].

The present work aims to extend the previously mentioned study of the catalytic properties of bimetallic Pd-Ni systems for CO oxidation and NO reduction reactions [12]. For this purpose, here the systems are examined under conditions closer to the real situation by including an additional reactant in the reaction mixture (propene as hydrocarbon) as well as by examining the catalytic behaviour of the systems after having been submitted to a thermal aging treatment. This latter is of a great practical relevance for this type of catalysts since, among the different causes of TWC deactivation, thermal degradation normally constitutes an irreversible characteristic [1,13], although some advances in this respect have been recently reported for particular catalyst configurations [14]. To achieve these goals, the catalytic behaviour of the systems was analysed as a function of the nature of the stoichiometric reactant mixture employed, the catalysts components (in particular, the influence of the presence of nickel and Ce-Zr mixed oxide) and the effects of thermal aging. In situ DRIFTS spectroscopy was employed to analyse the species chemisorbed under reaction conditions while yielding information on the evolution of the catalysts during the course of the catalytic experiments. XRD and HREM techniques were employed to explore the effects of the aging treatment on the catalysts, comparing the results with those reported in a former contribution in which the fresh systems were characterised in detail [11].

2. Experimental

Pure alumina (γ-Al_2O_3 Condea Puralox) and ceria-zirconia/alumina with 10 wt.% of Ce-Zr mixed oxide content (expressed, in accordance with ICP-AES analysis, as $Ce_{0.5}Zr_{0.5}O_2$) were employed as supports. The latter was prepared by equimolar cerium-zirconium coprecipitation within a reverse microemulsion containing the appropriate amount of alumina, followed by separation of the solid, rinsing with methanol, drying overnight at 393 K and calcining under air at 773 K for 2 h. Full details of the procedure and materials employed in this microemulsion preparation can be found elsewhere [8,15]. The supports were coimpregnated (incipient wetness method) with aqueous solutions of Pd(II) and Ni(II) nitrates (in order to achieve 1 wt.% loadings for each of the metals in the final catalysts) followed by overnight drying at 393 K and calcination under air at 773 K for 2 h. Supported monometallic Pd reference catalysts (with 1 wt.% loading) were prepared by the same method. S_{BET} values obtained for these catalysts were in all cases close to that of the parent alumina (ca. 200 $m^2\ g^{-1}$). The catalysts will be referred to as PdNiA and PdNiCZA (or using only a Pd prefix for the monometallic references) for the systems supported on alumina or ceria-zirconia/alumina, respectively. These catalysts were subjected to an accelerated aging treatment in a muffle furnace under air at 1273 K for 16 h. These latter will be denoted with a suffix a. S_{BET} values obtained for the aged catalysts were 84 and 83 $m^2\ g^{-1}$ for PdNiA-a and PdNiZCA-a, respectively.

Catalytic activity tests using a stoichiometric mixture of 1% CO + 0.1% C_3H_6 + 0.9% O_2 + 0.1% NO (N_2 balance) were performed in a pyrex glass fixed-bed flow reactor and are compared with those obtained under simpler stoichiometric mixtures of 1% CO + 0.5% O_2 and 1% CO + 0.45% O_2 + 0.1% NO (N_2 balance). Space velocity ($3 \times 10^4\ h^{-1}$; about 2.5 g of sample being employed) and sieving size (particles in the 0.125–0.250 mm range) were selected to minimize diffusion effects [12,16]. The gases were regulated with mass flow controllers and analysed using an on line Perkin-Elmer 1725X FTIR spectrometer coupled with a multiple reflection transmission cell (Infrared Analysis Inc.). Oxygen concentrations were determined with a paramagnetic analyser (Servomex 540A). Experimental error in the conversion values obtained under these conditions is estimated as ±7%. Prior to catalytic testing, an oxidation pretreatment was performed in situ under 2.5% O_2 (in N_2) flow at 773 K followed by cooling under the same atmosphere and a thorough N_2 purge at room temperature (RT). Tests were performed in the light-off mode, increasing the temperature under the reactive flow by employing a ramp of 5 K min^{-1} and using a glass-sheathed thermocouple placed in the centre of the catalyst bed for temperature control.

Diffuse reflectance infrared Fourier transform spectroscopy (DRIFTS) analysis of adsorbed species present on the catalyst surface under reaction conditions was carried out using a Perkin-Elmer 1750 FTIR fitted with an MCT detector. On-line analysis of the NO concentration at the outlet of the IR chamber was performed by chemiluminescence (Thermo Environmental Instruments 42C). The DRIFTS cell (Harrick) was fitted with CaF_2 windows and a heating cartridge that allowed samples to be heated to 773 K. Samples of ca. 65 mg were pretreated in situ under a diluted O_2 flow (in a similar manner described above for the catalytic tests), before introducing the reaction mixture and heating at 2 K min^{-1} from 298 to 673 K, recording one spectrum (4 cm^{-1} resolution, average of 50 scans) generally every 20–30 K. The gas mixture (similar to that employed for catalytic tests) was prepared using a computer-controlled gas-blender with 80 $cm^3\ min^{-1}$ passing through the catalyst bed.

Powder X-ray diffraction (XRD) patterns were recorded on a Seifert diffractometer using nickel-filtered Cu Kα radiation, operating at 40 kV and 40 mA, and with a 0.02–0.04° step size. A counting time of 5 s was employed. Analysis of the diffractograms and peak fittings were performed with the program Analyze RayfleX Version 2.293.

High resolution electron microscopy (HREM) images were recorded in a JEOL 2000 EX microscope, equipped with a top entry specimen holder, with 0.21 nm point to point resolution. The experimental micrographs were digitized using a CCD camera COHU-4910. Digital image processing was performed by using the SEMPER 6+ software.

3. Results and discussion

A previous paper reported in detail the main morphological/structural characteristics of PdNiA and PdNiCZA, focussing on the effect of the presence of Ni in the catalysts [11]; let us first give here a brief outline of the results obtained in that work since they could be of relevancy to explain catalytic properties of the systems [12]. Characterization at a nanoscopic level of these catalysts was achieved by employing mainly electron microscopy-related techniques (HREM, XEDS and STEM-EELS). In turn, that report extended previous studies which analysed the characteristics of the CZA support both at bulk and surface levels [17,18]. Analysis of the CZA support revealed the presence of rather homogeneous (in terms of compositional characteristics and structural/morphological properties) Ce-Zr mixed oxide nanoparticles (average size of ca. 3.4 nm) dispersed over the alumina support. Such Ce-Zr mixed oxide nanoparticles presented a pseudocubic (t″) or cubic (fluorite) phase (unfortunately, the low intensity of Raman bands did not allow unambiguous assignment of the phase of these nanoparticles while diffraction techniques cannot resolve this for such small particle sizes [11]) with lattice parameter in fair accordance with the nominal composition ($Ce_{0.5}Zr_{0.5}O_2$). Nanoprobe XEDS analysis of the PdNiCZA catalyst revealed a particular trend of palladium in interacting with the Ce-Zr mixed oxide component of the support. Noteworthy, this was shown to be indirectly favoured by the presence of nickel in the catalyst (no direct Pd-Ni interaction could be identified [11,12]). In contrast, nickel appeared to interact preferentially with the alumina component of the support (XEDS and FMR evidence). The chemical nature of the palladium and nickel components of the bimetallic catalysts was explored by XPS and XANES techniques [11,12]. These results showed that palladium appeared in the form of small PdO-type particles while nickel forms oxidic entities (of a NiO- or $NiAl_2O_4$-type, or both) in a very high-dispersed state (in accordance also with STEM-EELS evidence). The dispersion of Pd and the corresponding average size of the palladium particles appeared relatively similar for both PdNiA and PdNiCZA systems and displayed a value around 2.5 nm. Noteworthy, despite difficulties in obtaining direct observation in Z-contrast images of palladium particles interacting with the Ce-Zr mixed oxide in PdNiCZA, simultaneous recording of EELS spectra confirmed the presence of those particles, suggesting also a relatively large size (around 2 nm) for them.

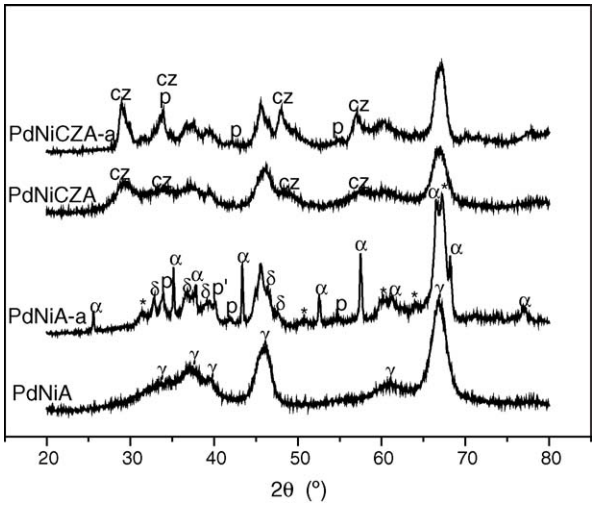

Fig. 1. X-ray diffractograms of the indicated samples; α, δ, and γ labels denote peaks characteristic of α-, δ-, and γ-Al_2O_3 phases while asterisk marks may correspond to δ- or θ-Al_2O_3 (note peaks of these latter are also coincident with those of γ-Al_2O_3 and appear also at positions close to those of the $NiAl_2O_4$ spinel see text); p and p′ correspond to PdO and metallic palladium phases while cz corresponds to phases related to the CZ component.

X-ray diffractograms of the bimetallic catalysts in their fresh and aged forms are shown in Fig. 1 while the main structural properties of these systems are summarised in Table 1. Analysis of the diffractograms of the fresh catalysts reveals the presence of features due exclusively to support constituents, thus indicating the relatively high degree of dispersion of the metallic components in the catalysts, in agreement with the above-mentioned studies [11]. Significant changes are observed as a consequence of the aging treatment and in association with the surface area loss (as indicated in Section 2). The γ-Al_2O_3 phase of the support is observed to be partially transformed into other transitional alumina phases, in particular α- and δ- (and/or θ-) aluminas, known to be stabilized at high temperatures in pure alumina (the γ phase transforms to δ at ca. 1000 K, θ at ca. 1200 K and α from 1273 K [19]). Comparison of the diffractograms of PdNiA-a and PdNiCZA-a reveals, as for the metal-free supports [20], that the presence of the Ce-Zr mixed oxide (CZ) hinders the transformation of the γ-Al_2O_3 into the α polymorph, being therefore most relevant in diminishing the effects of thermal degradation [20].

Table 1
Summary of structural characteristics of the Pd-Ni bimetallic catalysts as estimated from analysis of the X-ray diffractograms

Sample	Crystalline phases detected	CZ average particle size (nm)	CZ cell parameter (Å)
PdNiA	γ-Al_2O_3		
PdNiA-a	γ-Al_2O_3, δ- (and/or θ-) Al_2O_3, α-Al_2O_3, $NiAl_2O_4$, PdO, Pd		
PdNiCZA	γ-Al_2O_3, (Ce,Zr)O_x	3.0	$a_c \approx 5.29$
PdNiCZA-a	γ-Al_2O_3, δ- (and/or θ-) Al_2O_3, $NiAl_2O_4$, (Ce,Zr)O_x, PdO	13.0	$a_c \approx 5.29$, $a_c \approx 5.35$; $c_t \approx 5.26$, $a_t \approx 3.63$

Another apparent effect of the aging treatment is the appearance of peaks due to Pd-containing phases (PdO and metallic Pd), which implies the sintering of this component during aging. In contrast to PdNiA-a, metallic Pd appears to be absent in PdNiCZA-a, which suggests that the presence of CZ, along with the enhanced interaction of Pd with this component in the presence of Ni [11], favours the stabilization of oxidised states of palladium in the sintered particles. This observation is in agreement with previous proposals [21–23]. The influence of nickel on this effect is based on a comparison with the monometallic PdCZA catalyst in which some metallic Pd was detected after an aging treatment similar to the one performed here [23,24]. Regarding the effect of aging on the nickel component, the absence of peaks related to crystalline NiO eliminates an isomorphic sintering as a possibility for highly dispersed NiO-type entities that could be partially present in the fresh catalysts [11]. It may occur that nickel maintains the high level of dispersion presented in the fresh catalysts after aging [11]. However, the similarity between peaks of transitional alumina phases (in particular θ-Al_2O_3) and those of $NiAl_2O_4$ does not allow us to discard completely the possibility that nickel entities underwent a solid state reaction with alumina to form such a spinel phase [25]. In fact, DRIFTS experiments described below suggests that the nickel component also undergoes significant sintering during aging thus supporting that such nickel aluminate crystalline phase may be actually present in the aged catalysts (Table 1).

Another component which apparently transforms upon aging is the CZ. This is inferred from analysis of the peak at ca. 29° which reveals that this component not only sinters (Table 1) but also undergoes a compositional redistribution, as illustrated in more detail in Fig. 2. Thus, in addition to a central peak appearing at a value close to that observed for the fresh sample, two additional peaks are detected at either side. The position of the central peak (corresponding to a lattice parameter $a_c \approx 5.29$ Å, considering the (1 1 1) diffraction in the cubic fluorite- or pseudocubic t″ phase in which the CZ component crystallises for Ce/Zr ≥ ca. 1) is in reasonable agreement with an equimolar Ce and Zr composition in the CZ component [3,11], in accordance also with the chemical composition of the sample (see Section 2). It must be noted that this analysis must be considered carefully since, as a consequence of the nanosized nature of the crystals involved, uncertainties can appear in the estimation of compositional details from positions of the peaks in the X-ray diffractograms in these mixed oxide compounds [26]. This aside, the two lateral peaks indicate the presence of cerium-enriched (denoted as Cz in Fig. 2; lattice parameter $a_c \approx 5.35$ Å considering the (1 1 1) diffraction in the cubic cell, fairly consistent with a composition close to $Ce_{0.8}Zr_{0.2}O_2$) and zirconium-enriched (denoted as Zc in Fig. 2; lattice parameters $c_t \approx 5.26$ Å and $a_t = b_t \approx 3.63$ Å corresponding to the (1 0 1) diffraction in the tetragonal phase at which the mixed oxide compound crystallises below a certain Ce/Zr ratio [3,26] and which is fairly consistent with a composition close to $Ce_{0.2}Zr_{0.8}O_2$) phases. These observations are consistent with the occurrence of the phase partial segregation process during thermal ageing. The presence of nickel apparently favours the progress of this partial phase segregation according to a comparison between PdNiCZA-a and PdCZA-a (Fig. 2). This is almost certainly related to the mentioned favoured interaction between Pd and CZ in the Ni containing catalyst [11], since it is known that contact of CZ with a noble metal (in particular Pd) catalyses the phase segregation process [27], probably through facilitating the reduction of the cations (which in turn enhances their mobility) [3].

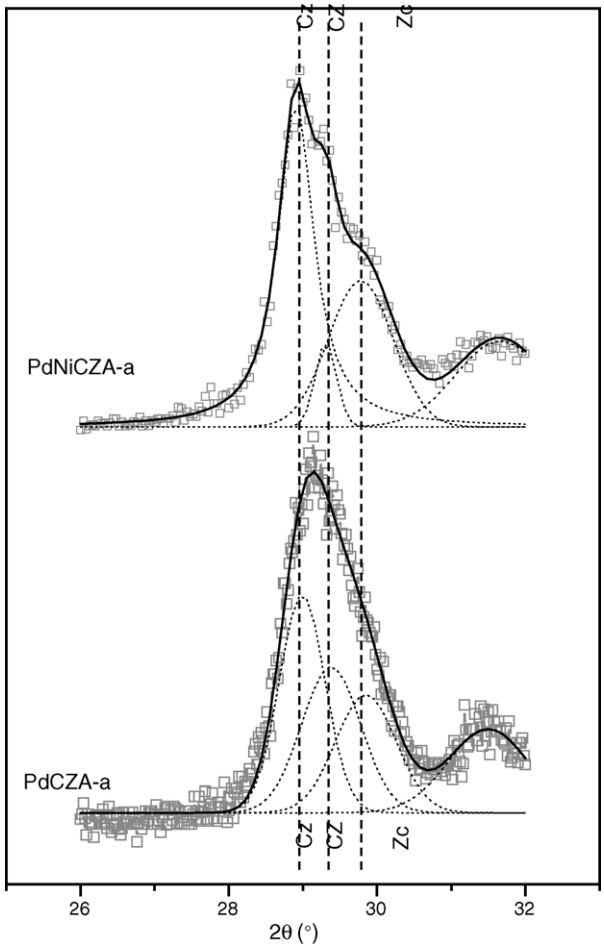

Fig. 2. Detail of the X-ray diffractograms of the indicated samples and results of the fittings using pseudo-Voigt functions. Vertical lines mark positions of the peak corresponding to Ce-enriched (Cz), equimolar (CZ) and Zr-enriched phases (Zc) of the CZ component (see text for details).

Results of the catalytic activity tests under the $CO + O_2 + NO + C_3H_6$ stoichiometric mixture for the fresh and aged bimetallic Pd-Ni catalysts are shown in Fig. 3. Comparison between the catalytic performances of fresh and aged catalysts reveals the detrimental effect of the aging treatment on the conversion of the three pollutants. In accordance with the characterization results (Fig. 1 and Table 1), and in agreement with previous proposals [13,23,28], this can be related to the sintering of both palladium and CZ which decreases both the number of active centres at the surface of palladium and the number of interactions between Pd and CZ. This latter is particularly relevant for the CO oxidation reaction, according to the well known promoting effect of CZ for this reaction [2].

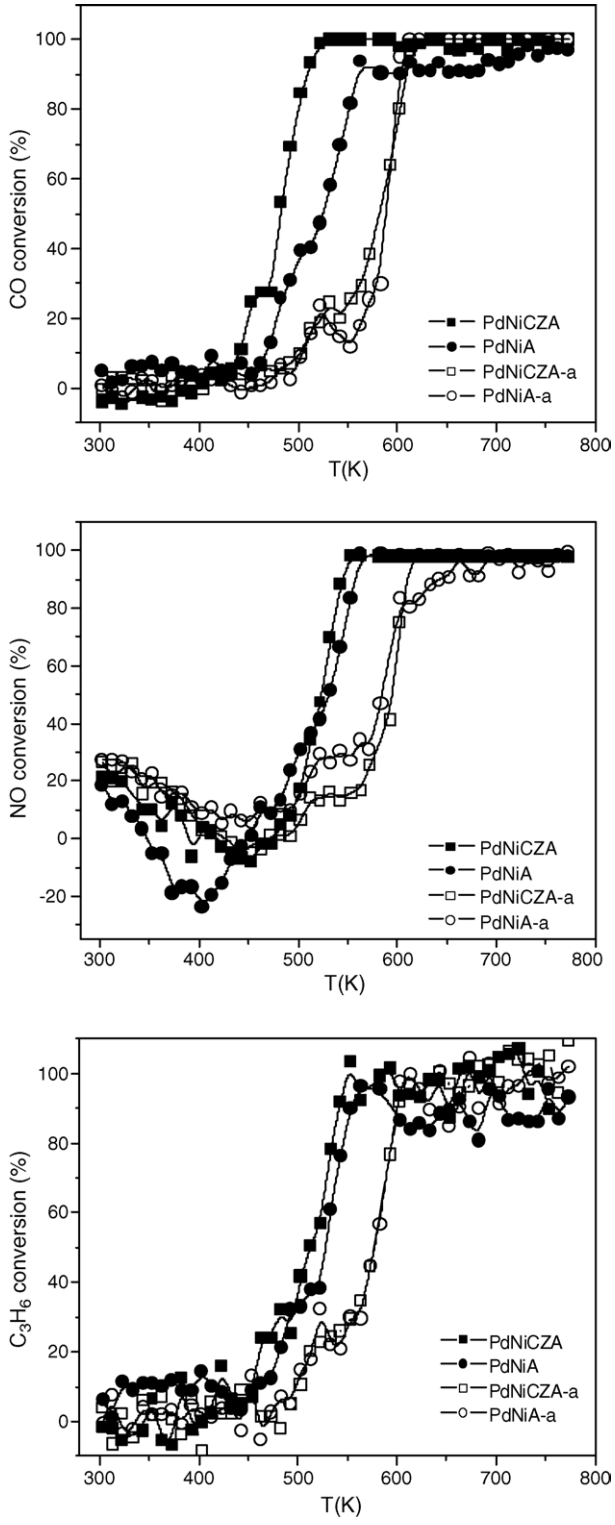

Fig. 3. Conversion profiles for CO (top), NO (middle) and C_3H_6 (bottom) obtained during the catalytic measurements under stoichiometric CO + O_2 + NO + C_3H_6 gas mixture for the indicated catalysts.

This, along with possible detrimental effects of increasing the particle size of the CZ promoter [12,23], can explain the relatively small differences between the two aged catalysts for this reaction. Concerning selectivity to N_2 during NO reduction (not shown), no important differences were detected between

Table 2
Isoconversion temperatures (in K) at 50% conversion for the three pollutants obtained during light-off tests under stoichiometric conditions at 3×10^4 h^{-1} GHSV for the reactions A = CO + O_2, B = CO + O_2 + NO and C = CO + O_2 + NO + C_3H_6 over the indicated catalysts

	T_{50} (CO)			T_{50} (NO)		T_{50} (C_3H_6)
	A	B	C	B	C	C
PdNiCZA	334	403	482	455	524	511
PdNiA	447	479	526	408	531	528
PdNiCZA-a	463	518	581	525	595	576
PdNiA-a	469	518	588	533	584	577

fresh and aged catalysts. In any of the cases and in contrast to results obtained with simpler CO + O_2 + NO reaction mixture [12], relatively low amounts of N_2O were formed (lower than ca. 15% of the NO reduced and decreasing with increasing reaction temperature), which may be due to the relatively high reaction temperature observed in the presence of the hydrocarbon (see below).

Comparing the conversion curves of the two fresh catalysts reveals only minor differences resulting from the presence of CZ. Thus, both NO reduction, taking place above ca. 420–450 K (note low temperature data are affected by adsorption/desorption effects [8,12]) and C_3H_6 oxidation show fairly similar conversion curves (onset of NO reduction occurring at slightly lower temperature for PdNiA), while only CO conversion is apparently promoted by the CZ component. This contrasts with results observed during light-off tests with simplified CO + O_2 or CO + O_2 + NO stoichiometric mixtures [12]. Data collected in Table 2 reflect these differences. It is quite apparent that the existence of competition between the different reactants affects significantly the catalytic performance for CO oxidation and NO reduction. In particular, in the case of CO oxidation, it is clear (Table 2) that as the reactant mixture becomes more complex by addition of reactants (first NO and then C_3H_6) the catalytic activity, as well as the extent of the promoting effect of CZ, gradually diminishes. In the case of NO reduction, introduction of C_3H_6 produces a decrease in the catalytic activity and affects to a greater extent the PdNiA catalyst, which was the most active under CO + O_2 + NO.

In order to explore these aspects, the catalysts were examined by DRIFTS spectroscopy under reaction conditions. Since a recent report has examined the effects of introducing NO into the CO + O_2 reactant mixture [12], we will focus our attention here on the effects of the presence of the hydrocarbon. Spectra obtained under the full reactant mixture for the two fresh catalysts are shown in Figs. 4 and 5. A reasonable correlation is observed between the evolution of CO_2(g) (and loss of CO(g) giving the two bands centred at 2143 cm^{-1}) and CO conversion values observed during the catalytic tests (Fig. 3). Unfortunately, the lower concentrations (and smaller molar absorption coefficients) of NO(g) and C_3H_6(g) do not allow direct monitoring of the evolution of these gases in the FTIR spectra. However, on-line chemiluminescence monitoring of NO in the outlet of the DRIFTS cell showed reasonable agreement with conversion values observed for this reactant

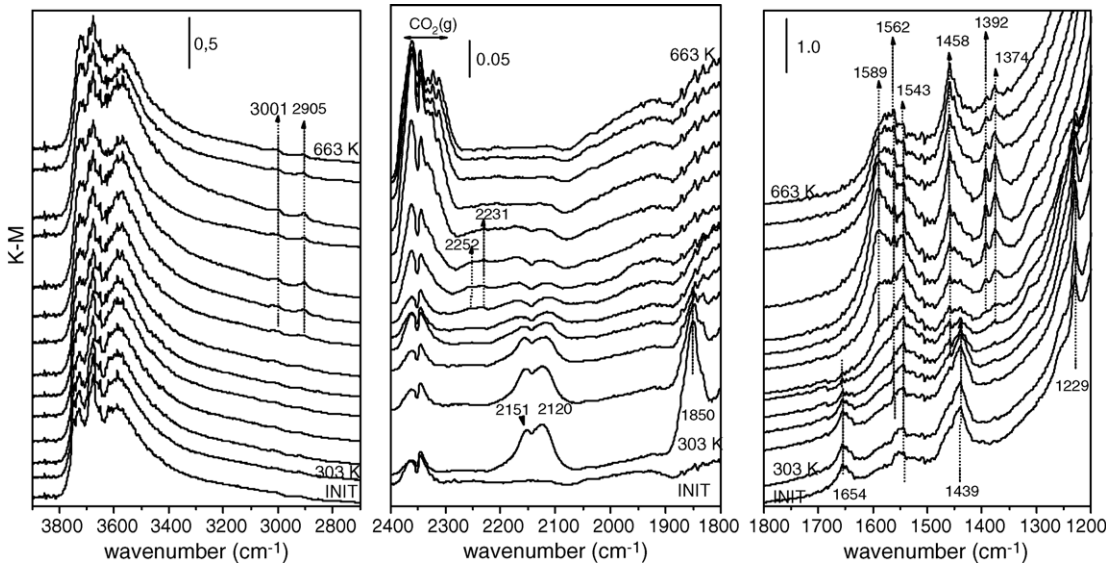

Fig. 4. In situ DRIFTS spectra of the PdNiCZA catalyst. The spectrum at the bottom corresponds to the initial calcined catalyst prior to admission of the reactant mixture. Subsequent spectra were recorded under stoichiometric CO + O_2 + NO + C_3H_6 gas mixture from 303 K (bottom) to 663 K (top) every 30 K (from bottom to top).

(Fig. 3). These correlations between the reactivity observed in the DRIFTS cell and the data obtained in the reaction vessel, allow a direct link between observations made by DRIFTS and the activity data. A band around 1850 cm^{-1}, attributed to nitrosyl species chemisorbed on Ni^{2+} cations [12,29,30], is observed immediately upon contact with the reactant mixture for both catalysts. In turn, bands at 2151 and 2120 cm^{-1} for PdNiCZA (Fig. 4) and a relatively weaker broad band centred at 2134 cm^{-1} for PdNiA [31,32] (Fig. 5), due to carbonyl species chemisorbed on oxidised Pd^{n+} entities, are also formed upon initial contact. At intermediate temperatures, bands due to carbonyl species chemisorbed on metallic palladium (at 2095 cm^{-1}, red-shifting from 453 K, attributable to atop species [33–35], and at 1970 cm^{-1} with a relatively broad lower frequency shoulder extending to ca. 1850 cm^{-1}, attributable to bridging or bridging and three-fold species [33–35]) are apparent for PdNiA (Fig. 5). It may be noted that the onset of the red shift in the atop carbonyl band is in good agreement with the initiation of CO oxidation (Fig. 3), thus providing evidence for a Langmuir–Hinshelwood kinetic scheme in which this reaction takes place over PdNiA, as detailed elsewhere [12,35]. The presence of metallic palladium carbonyls is not so clear in the case of PdNiCZA although weak bands at ca. 2100–2050 and 1980–1850 cm^{-1} reveal their

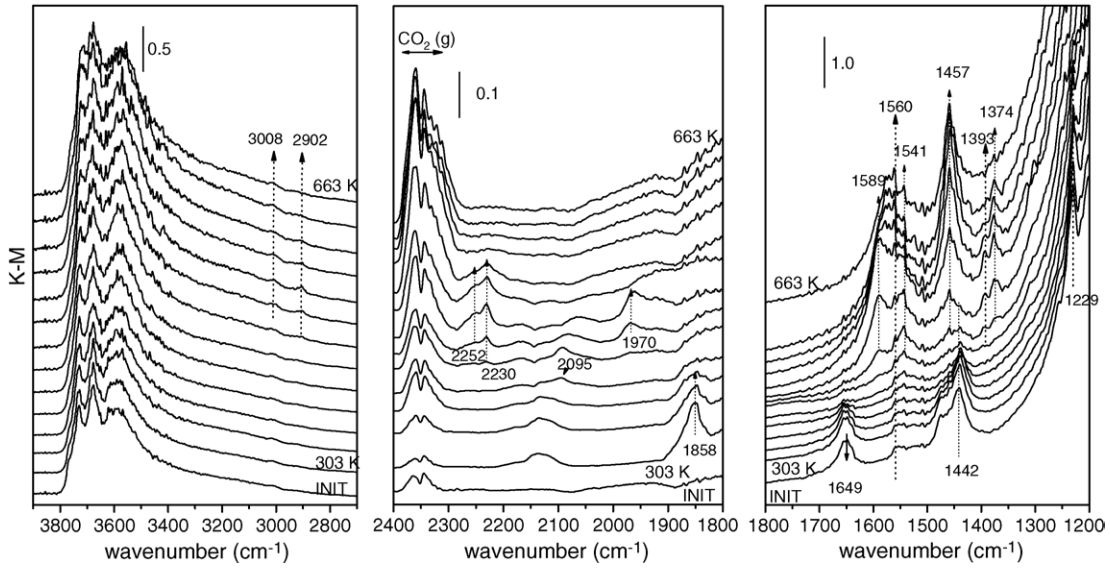

Fig. 5. In situ DRIFTS spectra of the PdNiA catalyst. The spectrum at the bottom corresponds to the initial calcined catalyst prior to admission of the reactant mixture. The remainder correspond to spectra recorded under stoichiometric CO + O_2 + NO + C_3H_6 gas mixture from 303 K (bottom) to 663 K (top) every 30 K (from bottom to top).

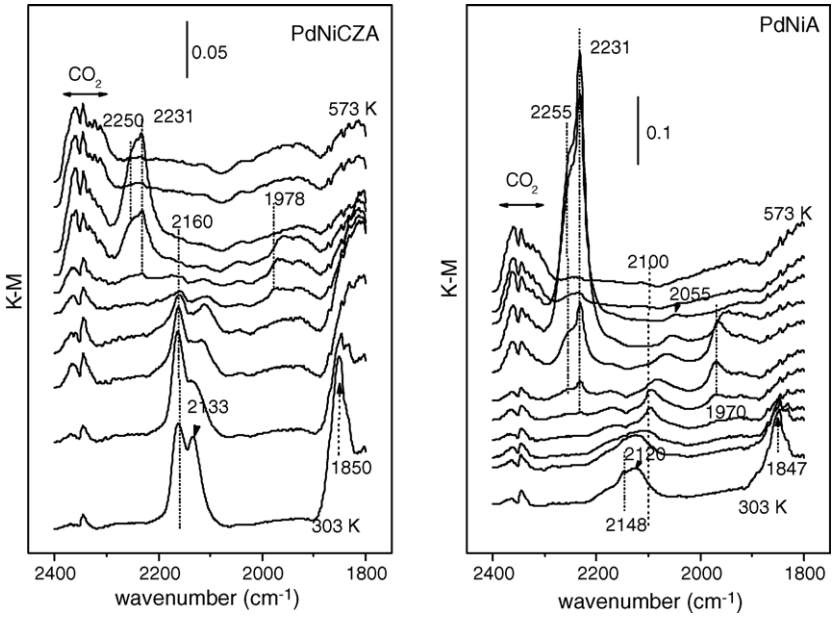

Fig. 6. In situ DRIFTS spectra of the indicated catalysts recorded every 30 K under a stoichiometric CO + O_2 + NO gas mixture from 303 to 573 K (from bottom to top).

presence at fairly similar reaction temperatures as those observed for PdNiA and thus indicate the formation of metallic palladium particles in the course of the reaction. Additionally, bands due to isocyanate species chemisorbed on alumina (at ca. 2252 and 2230 cm^{-1} [35–37]) appear from ca. 423 K (concurrent with the onset of NO reduction, Fig. 3), disappearing at $T \geq 573$ K.

Comparison with similar experiments performed in the absence of C_3H_6 (Fig. 6) reveals that the presence of the hydrocarbon hinders the formation of carbonyl species over the palladium particles, the extent of this effect being most apparent for PdNiCZA. Lesser intensity of bands due to isocyanate species is also apparent when propene is present. These results are in line with previous observations for monometallic Pd catalysts and can be attributed to the favourable chemisorption of propene, or fragments derived from its decomposition, over the palladium particles while in competition with the other reactants [24]. Such favoured hydrocarbon chemisorption decreases the amount of free sites for the adsorption of either CO or NO over the active Pd metallic particles, thus preventing their activation for the respective reactions. The hydrocarbon, therefore, induces a self-poisoning that can be considered as the main effect responsible for the lower CO oxidation or NO reduction activity when it is present in the reactant mixture (Table 2). The greater hindrance to CO chemisorption for PdNiCZA in the presence of the hydrocarbon apparently has a stronger relative effect on the CO oxidation capability of this system compared with PdNiA (Table 2). It must be noted, however, that a bifunctional mechanism is operative for PdNiCZA for this reaction (with both Pd and CZ being involved [2,12,38]), while the palladium particles alone are the active phase in PdNiA [12]. The fact that the former still maintains an appreciable CZ promoting effect for this reaction while the CO and C_3H_6 conversion profiles appear fairly matched for the latter catalyst suggests, as inferred from results reported below, that the hydrocarbon self-poisoning only influences the CZ component to a limited extent and therefore allows some degree of operation over this main component [12]. It must be noted in this respect that the onset of the C_3H_6 oxidation indicates that the hydrocarbon has been activated, subsequently reacted with oxygen and further desorbed as CO_2, therefore suggesting that the magnitude of the self-poisoning effect must be limited above this reaction temperature. This accounts for the correlation between conversion curves for both reactants. In the case of NO reduction, the presence of the hydrocarbon influences PdNiA to a relatively greater extent (Table 2). The high degree of similarity between NO conversion profiles for both catalysts and between these and the respective C_3H_6 conversion curves (Fig. 3 and Table 2) should be noted. This provides a strong indication that the self-poisoning by the hydrocarbon mainly affects the palladium particles, in accordance with the fact that the rate determining step for this reaction in any of these catalysts is mainly related to NO adsorption-dissociative activation steps taking place over such particles [2,12,35,39]. Indications of the more limited NO reactivity in the presence of propene are provided by the lower comparative intensity of the bands due to isocyanate species in this case (compare Figs. 4 and 5 with Fig. 6), taking into account that these species are proposed to form following NO dissociation on the metallic palladium particles and subsequent N–CO reaction and spillover onto the alumina support where they accumulate [32,36,40,41].

Analysis of the 1800–1200 cm^{-1} region of the spectra in Figs. 4 and 5 reveals the presence of bands at 1654–1649, 1442–1439 and 1229 cm^{-1} (due to bicarbonate species chemisorbed on alumina [42,43]) and at ca. 1545 and 1460 cm^{-1} which may correspond to carboxylate species chemisorbed on alumina [44], which are present prior to introduction of the reactant

mixture. The growth of a band at 1543–1541 cm^{-1}, that may correspond to carbonate or nitrate species chemisorbed on alumina [12,45] (in accordance with its detection under $CO + O_2 + NO$ reaction conditions [12]), is observed from relatively low reaction temperatures. Bands characteristic of the presence of propene in the reactant mixture are those appearing at intermediate reaction temperature at 1589, 1392 and 1374 cm^{-1} (which along with those at 3001 and 2905–2902 cm^{-1} correspond to formate species chemisorbed on the alumina [24,46]) and those at ca. 1560 and 1457 cm^{-1} (attributed to acrylate or acetate species chemisorbed on alumina [43,44,47]). These latter species display a higher thermal stability under reaction conditions than formate species, in agreement with previous results [48]. In principle, none of the bands detected in the spectra are related to propene (or fragments derived from its decomposition) on the palladium particles. Only a weak band appearing at ca. 1310 cm^{-1} from relatively low reaction temperature may correspond to $-CH_3$ fragments, in accordance with a previous study [24]. However, in contrast to that study [24], the weakness of this band in the spectra of Figs. 4 and 5 does not allow us to discard fully the possibility that this band could be related to one of the modes of chemisorbed nitrate species [12]. Nevertheless, as noted previously [24], it must be taken into account that the observation of infrared active vibration modes of propene or derived species chemisorbed over the metallic Pd particles formed in the course of the reaction can be strongly hindered as a consequence of the normal dipole surface selection rule [49].

Spectra similar to those presented in Figs. 4 and 5 were recorded under the same conditions for the two aged catalysts (results not shown). In contrast to results observed for the fresh catalysts, bands attributable to species chemisorbed on the palladium particles were barely observable in the spectra, as expected given the strongly sintered state of the metal according to characterization results (Fig. 1). Under these conditions, it becomes quite difficult to extract conclusions related to the catalytic behaviour from these spectra. It is noteworthy that, in contrast to experiments performed over the fresh systems (Figs. 4 and 5), nitrosyl species chemisorbed on Ni^{2+} cations were not detected for the aged catalysts. This suggests that the nickel component also underwent significant sintering by forming nickel aluminate crystals, as suggested above. In this respect, it may be noted that formation of such crystals in PdNiCZA must be favoured by the strong preference of Ni towards interaction with the alumina component of this catalyst [11].

DRIFTS spectra recorded to determine the state of the catalyst at the end of the run under $CO + O_2 + NO + C_3H_6$ by using CO as probe molecule are displayed in Fig. 7. Bands due to carbonyls chemisorbed on metallic palladium particles are mainly observed for the two fresh systems (atop carbonyls at 2092 cm^{-1} and bridging CO or adsorption at bridging and three-fold hollow sites at ca. 1983 and 1920 cm^{-1} respectively) while weaker bands due to carbonyls chemisorbed on oxidised Pd^{n+} (bands at 2149 or 2141 cm^{-1}) show contributions to the spectra (particularly for PdNiCZA). These spectra reveal that in these catalysts palladium forms predominantly metallic palladium particles at the end of the reaction, which are

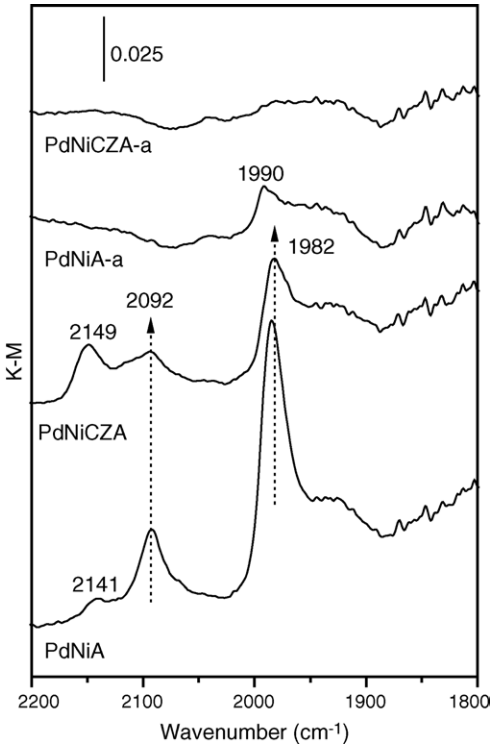

Fig. 7. DRIFTS spectra of the indicated catalysts recorded after cooling to 303 K under nitrogen at the end of the $CO + O_2 + NO + C_3H_6$ reaction, followed by treatment under a flow of 3% CO in nitrogen and final purging under nitrogen at 303 K.

partially oxidised as a consequence of interaction with NO [12,32]. Stabilization of a partially oxidised state of palladium in PdNiCZA can also be a consequence of the presence of propene and its influence over particles in contact with the CZ component [50]. In contrast, the aged systems display carbonyl bands of very low intensity, which are a consequence of the sintering of palladium. In particular, chemisorbed carbonyls are barely observable for PdNiCZA-a. In order to confirm whether palladium encapsulation occurred, this catalyst has been analysed by HREM focussing on clarifying this particular situation. This type of phenomena has been observed upon severe aging or under SMSI conditions in this type of systems [13,51] and could be responsible (even if only partially) for the residual carbonyl intensity observed in the post-reaction experiment for PdNiCZA-a (Fig. 7). Indeed, experimental evidence of the occurrence of this phenomenon is shown in Fig. 8. The digital diffraction pattern performed inside the encapsulated particle shows spacings of 2.20 and 2.17 Å forming an angle of 70°, typical of metallic palladium while the layer over the particle shows spacings of 2.55 Å, typical of the (0 0 2) plane of the fluorite structure of the CZ component (see XRD discussion above). This is probably best appreciated in the intensity profile carried out by following the white line marked on the HREM picture and in which the various spacings observed in the micrograph are depicted.

Finally, we analyse the influence of the presence of nickel and of the aging treatment on the catalytic activity using the full reactant mixture over the CZA-supported samples (full details

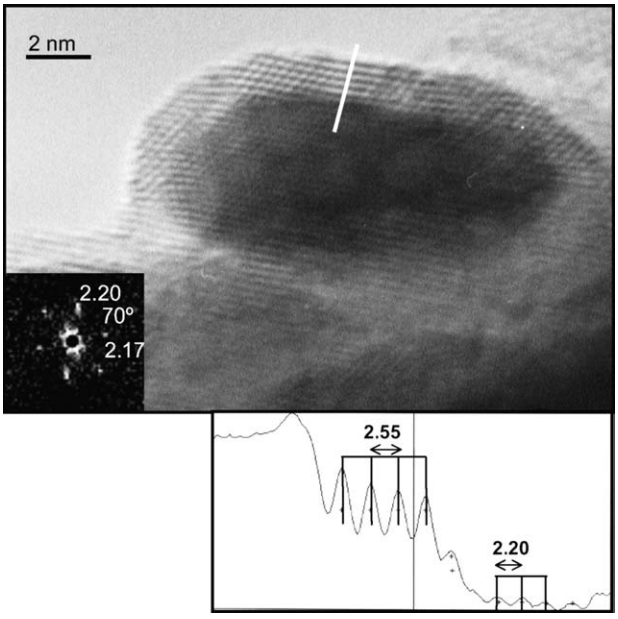

Fig. 8. (Top) HREM image of a palladium particle encapsulated by the CZ component of the support in PdNiCZA-a; the inset shows the digital diffraction pattern performed inside the palladium particle. (Bottom) Intensity profile along the line marked in the HREM image, showing spacings typical of CZ and metallic palladium (see text).

of the monometallic Pd systems can be found elsewhere [24]). A general benefit is obtained from the presence of nickel in the fresh systems while the opposite occurs for the aged samples (Fig. 9). Considering that nickel must not be directly involved in the catalytic activity of the system (in terms of providing active sites for the reactions) and that no evidence of interactions between nickel and palladium was found in PdNiCZA [11,12], the differences must be related to the nickel-induced changes in the palladium distribution over the catalysts [11]. As described above, this is related to a preferred interaction between palladium and CZ which increases the amount of active Pd-CZ interface sites in the bimetallic catalyst with respect to the monometallic one.

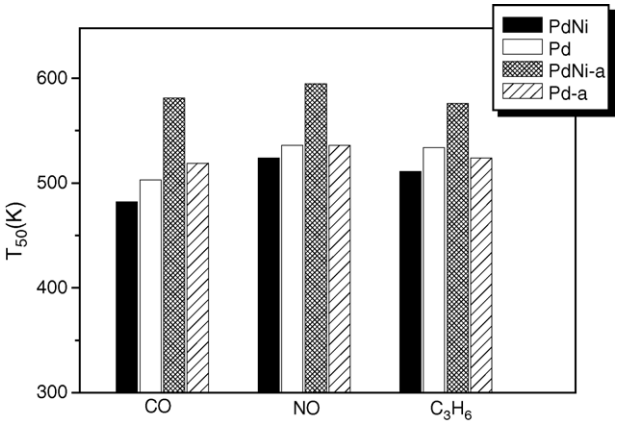

Fig. 9. Isoconversion temperatures at 50% conversion for the three pollutants obtained during light-off tests under stoichiometric conditions at a GHSV of $3 \times 10^4\ h^{-1}$ over the indicated CZA-supported catalysts.

Such an effect can benefit the catalytic performance by directly enhancing the CO oxidation activity in the bifunctionally operating Pd-CZ system, in accordance with the discussion above. In turn, the enhancement in hydrocarbon oxidation activity for such Pd-CZ entities is in line with recent results and has been attributed to a stabilization of partially oxidised palladium states which are particularly active for this reaction [50]. This can in turn affect the NO reduction activity as a consequence of decreasing the hydrocarbon self-poisoning effect. However, the greater thermal degradation of the CZ component (Fig. 2) and the possibility that the encapsulation phenomena are maximised for such Pd-CZ interactions (Fig. 8) may be the main factors that negatively affect the performance of the aged bimetallic catalyst. Note in this sense that a previous analysis, similar to that in Fig. 7, of the aged monometallic Pd system indicated that although palladium also suffered a significant degree of sintering, a greater amount of palladium remained exposed [24].

4. Conclusions

Bimetallic Pd-Ni catalysts supported on Al_2O_3 and $(Ce,Zr)O_x/Al_2O_3$ were examined for the elimination of CO, NO and C_3H_6 under stoichiometric conditions. The influence of a thermal aging treatment at 1273 K, the presence of nickel in the $(Ce,Zr)O_x/Al_2O_3$-supported system and the effect of introducing the hydrocarbon into the reactant mixture were analysed. The aging induces a significant sintering of the catalyst that affects all of its components. While, in accordance with previous reports [20], the presence of CZ hinders the thermal degradation of the alumina support, the preferred interaction between Pd and the Ce-Zr mixed oxide in the bimetallic catalyst (indirectly favoured by the presence of nickel [11,12]) apparently induces a greater extent of phase segregation of the equimolar Ce-Zr mixed oxide component into the more thermodynamically stable Ce- and Zr-enriched phases. Additionally, the encapsulation of palladium particles by Ce-Zr mixed oxide entities was observed by HREM. These factors stand out as being mainly responsible for the poorer catalytic performance generally observed for the aged $(Ce,Zr)O_x/Al_2O_3$-supported bimetallic system. Therefore, the same phenomenon that benefits the activity of the fresh catalyst (favoured formation of Pd-CZ contacts in the presence of nickel [11,12]) appears detrimental for the performance of the aged one (as a consequence of the greater degree of CZ phases segregation and Pd encapsulation by CZ). Finally, analysis by DRIFTS reveals the presence of significant competition between the reactants that explains the decreasing activities upon increasing the complexity of the reactant mixture. In particular, a self-poisoning effect by the hydrocarbon has been highlighted and related to hindered chemisorption of CO and NO, affecting most specifically the active palladium particles.

Acknowledgements

A.B.H. wishes to thank the Comunidad de Madrid for financial support through a Ph.D. grant and the program

''Ayudas para estancias breves en centros de investigación extranjeros''. Financial support by CICyT project MAT2000-1467 is acknowledged.

References

[1] E.S.J. Lox, B.H. Engler, in: G. Ertl, H. Knözinger, J. Weitkamp (Eds.), Environmental Catalysis, Wiley-VCH, 1999, p. 1.
[2] A. Martínez-Arias, J.C. Conesa, M. Fernández-García, J.A. Anderson, in: J.A. Anderson, M. Fernández-García (Eds.), Supported Metals in Catalysis, Imperial College Press, 2005, p. 283.
[3] J. Kašpar, P. Fornasiero, in: A. Trovarelli (Ed.), Catalysis by Ceria and Related Materials, Imperial College Press, 2002, p. 217.
[4] R. van Yperen, D. Lindner, L. Mubmann, E.S. Lox, T. Kreuzer, Stud. Surf. Sci. Catal. 116 (1998) 51.
[5] J.F. Trillat, J. Massadier, B. Morawek, H. Praliaud, A.J. Renouprez, Stud. Surf. Sci. Catal. 116 (1998) 103.
[6] A. El Hamdaoui, G. Bergeret, J. Massadier, M. Primet, A.J. Renouprez, J. Catal. 148 (1994) 47.
[7] M. Fernández-García, A. Martínez-Arias, C. Belver, J.A. Anderson, J.C. Conesa, J. Soria, J. Catal. 190 (2000) 387.
[8] A.B. Hungría, A. Iglesias-Juez, A. Martínez-Arias, M. Fernández-García, J.A. Anderson, J.C. Conesa, J. Soria, J. Catal. 206 (2002) 281.
[9] S. Yamamoto, K. Matsushita, Nippon Kagaku Kaishi (2000) 553.
[10] S. Yamamoto, K. Matsushita, Y. Hanaki, Nippon Kagaku Kaishi (2001) 19.
[11] A.B. Hungría, N.D. Browning, R.P. Erni, M. Fernández-García, J.C. Conesa, J.A. Pérez-Omil, A. Martínez-Arias, J. Catal. 235 (2005) 251–261.
[12] A.B. Hungría, M. Fernández-García, J.A. Anderson, A. Martínez-Arias, J. Catal. 235 (2005) 262–271.
[13] M. Shelef, G.W. Graham, R.W. McCabe, in: A. Trovarelli (Ed.), Catalysis by Ceria and Related Materials, Imperial College Press, 2002, p. 343.
[14] N. Hickey, P. Fornasiero, R. Di Monte, J. Kašpar, J.R. González-Velasco, M.A. Gutiérrez-Ortiz, M.P. González-Marcos, J.M. Gatica, S. Bernal, Chem. Commun. (2004) 196.
[15] A. Martínez-Arias, M. Fernández-García, V. Ballesteros, L.N. Salamanca, C. Otero, J.C. Conesa, J. Soria, Langmuir 15 (1999) 4796.
[16] R. Cataluña Veses, Ph.D. Thesis, Universidad Politécnica de Madrid, 1995.
[17] M. Fernández-García, A. Martínez-Arias, A. Iglesias-Juez, C. Belver, A.B. Hungría, J.C. Conesa, J. Soria, J. Catal. 194 (2000) 385.
[18] A. Martínez-Arias, M. Fernández-García, A.B. Hungría, J.C. Conesa, J. Soria, J. Alloys Compd. 323–324 (2001) 605.
[19] I. Levin, D. Brando, J. Am. Ceram. Soc. 81 (1998) 1995.
[20] M. Fernández-García, A. Martínez-Arias, A.B. Hungría, A. Iglesias-Juez, J.C. Conesa, J. Soria, Phys. Chem. Chem. Phys. 4 (2002) 2473.
[21] A. Trovarelli, Catal. Rev. Sci. Eng. 38 (1996) 439, and references therein.
[22] S. Yamamoto, K. Matsushita, Y. Hanaki, Nippon Kagaku Kaishi (2001) 205.
[23] A. Iglesias-Juez, A. Martínez-Arias, M. Fernández-García, J. Catal. 221 (2004) 148.
[24] A. Martínez-Arias, M. Fernández-García, A.B. Hungría, A. Iglesias-Juez, K. Duncan, R. Smith, J.A. Anderson, J.C. Conesa, J. Soria, J. Catal. 204 (2001) 238.
[25] C. Otero Areán, J.S. Díez Viñuela, J. Sol. St. Chem. 60 (1985) 1.
[26] R. Di Monte, J. Kašpar, J. Mater. Chem. 15 (2005) 633.
[27] K. Kenevey, F. Valdivieso, M. Soustelle, M. Pijolat, Appl. Catal. B 29 (2001) 93.
[28] R.A. Daley, S.Y. Cristou, A.M. Efstathiou, J.A. Anderson, Appl. Catal. B. 60 (2005) 119.
[29] J.B. Peri, J. Catal. 86 (1984) 84.
[30] G. Niu, Y. Huang, Z. Cao, Y. Huang, Q. Li, Appl. Surf. Sci. 141 (1999) 35.
[31] X. Xu, D.W. Goodman, J. Phys. Chem. 97 (1993) 7711.
[32] A. Martínez-Arias, M. Fernández-García, A. Iglesias-Juez, A.B. Hungría, J.A. Anderson, J.C. Conesa, J. Soria, Appl. Catal. B 31 (2001) 51.
[33] X. Xu, P. Chen, D.W. Goodman, J. Phys. Chem. 98 (1994) 9242.
[34] I.V. Yudanov, R. Sahnoun, K.M. Neyman, N. Rösch, J. Hoffmann, S. Schauermann, V. Johánek, H. Unterhalt, G. Rupprechter, J. Libuda, H.-J. Freund, J. Phys. Chem. B 107 (2003) 255.
[35] A. Martínez-Arias, A.B. Hungría, M. Fernández-García, A. Iglesias-Juez, J.A. Anderson, J.C. Conesa, J. Catal. 221 (2004) 85.
[36] F. Solymosi, J. Sarkany, A. Schauer, J. Catal. 46 (1977) 297.
[37] K. Almusaiteer, S.C. Chuang, J. Catal. 184 (1999) 189.
[38] M. Fernández-García, A. Martínez-Arias, A. Iglesias-Juez, A.B. Hungría, J.A. Anderson, J.C. Conesa, J. Soria, Appl. Catal. B 31 (2001) 39.
[39] L. Piccolo, C.R. Henry, J. Mol. Catal. A 167 (2001) 181.
[40] F. Solymosi, J. Rasko, J. Catal. 63 (1980) 217.
[41] N. Macleod, R.M. Lambert, Chem. Commun. (2003) 1300.
[42] A.M. Turek, I.E. Wachs, E. DeCanio, J. Phys. Chem. 96 (1992) 5000.
[43] A. Martínez-Arias, M. Fernández-García, A. Iglesias-Juez, J.A. Anderson, J.C. Conesa, J. Soria, Appl. Catal. B 28 (2000) 29.
[44] J.A. Anderson, C.H. Rochester, J. Chem. Soc., Faraday Trans. 85 (1989) 1117.
[45] A.A. Davydov, in: C.H. Rochester (Ed.), Infrared Spectroscopy of Adsorbed Species on the Surface of Transition Metal Oxides, John Wiley & Sons., 1990, p. 75.
[46] G. Busca, J. Lamotte, J.C. Lavalley, V. Lorenzelli, J. Am. Chem. Soc. 109 (1987) 5197.
[47] K. Shimizu, H. Kawabata, A. Satsuma, T. Hattori, J. Phys. Chem. B 103 (1999) 5240.
[48] D.K. Captain, M.D. Amiridis, J. Catal. 184 (1999) 377.
[49] R.F. Willis, A.A. Lucas, G.D. Mahan, in: D.A. King, D.P. Woodruff (Eds.), The Chemical Physics of Solid Surfaces and Heterogeneous Catalysis, vol. 2, Elsevier, 1983, p. 59.
[50] M. Fernández-García, A. Iglesias-Juez, A. Martínez-Arias, A.B. Hungría, J.A. Anderson, J.C. Conesa, J. Soria, J. Catal. 221 (2004) 594.
[51] S. Bernal, J.J. Calvino, J.M. Gatica, C. López Cartes, J.M. Pintado, in: A. Trovarelli (Ed.), Catalysis by Ceria and Related Materials, Imperial College Press, 2002, p. 85.